

Experimental Analysis of a Wideband Pattern Diversity Antenna With Compact Reconfigurable CPW-to-Slotline Transition Feed

Yue Li, Zhijun Zhang, *Senior Member, IEEE*, Jianfeng Zheng, Zhenghe Feng, *Senior Member, IEEE*, and Magdy F. Iskander, *Fellow, IEEE*

Abstract—A wideband antenna with a reconfigurable coplanar waveguide (CPW)-to-slotline transition feed is proposed for pattern diversity applications. The feed provides three modes -CPW feed, left slotline (LS) feed and right slotline (RS) feed- without extra matching structures. Changes between modes are controlled by only two p-I-n diodes. Features of the proposed switchable feed include compact size and simple bias circuit. The equivalent transmission line model is used in the analysis of the proposed design. A prototype of the proposed antenna is fabricated, tested, and the obtained results including reflection coefficient, radiation patterns and gains, are present. A measurement of channel capacity is carried out to prove the benefit of pattern diversity when using the proposed antenna in both line-of-sight (LOS) and non-line-of-sight (NLOS) communication scenarios.

Index Terms—Antenna feed, channel capacity, pattern diversity, reconfigurable antennas, wideband antennas.

I. INTRODUCTION

WITH the rapid progress in developing advanced wireless communication systems, the advantages of using reconfigurable antenna patterns have been recognized and widely adopted in many designs. Reconfigurable antenna patterns provide pattern diversity that could be used to provide dynamic radiation coverage and mitigate multi-path fading. The diversity and increased directional gains of pattern reconfigurable antennas also improves coverage and increase the channel capacity, especially in the multiple antennas system [1]–[3]. Among the recent designs of such antenna systems is the research work published in [4]–[13]. One method to achieve reconfigurable pattern is to adjust the structure of the radiating

element, including the antenna shape [4], [5], shorting sections [6] and parasitic elements [7], [8], dynamically. Another reconfigurable pattern solution may be achieved through the selection of the radiating elements [9]–[13]. In this case, radiating elements in different directions are electronically selected by switchable mechanism to achieve the desired directive beams [9]–[11].

In [12], [13], a reconfigurable CPW-to-slotline transition is proposed and a compact antenna feed, supporting both the CPW and slotline feed is described. Such a transition presents an effective solution to the feeding of different radiating elements in a relatively compact dimension. Such a feed approach has been widely studied and applied in different configurations [12]–[16]. For example, in the design described in [14], the CPW feed was converted to slotline feed by adding a 180° phase shifter. Another method to design CPW-to-slotline transition is to short circuit one of the two slots of the CPW, and add a $\lambda/4$ transformer structure to avoid reflections from the shorted end and provide good impedance matching [12], [13], [15]. In [13], the matching slot was used as a radiating element, while a function similar to a transformer was realized in [16] by using a CPW series stub printed at the center conductor of the CPW. All the designs reported in [12]–[16] required extra structures for mode convergence, including $\lambda/2$ phase shifter [14] and $\lambda/4$ matching structures [12], [13], [15], which occupy considerable space in the feed network.

In this paper, a compact switchable CPW-to-slotline transition without any extra structures is proposed and can be treated as an improvement from the design reported in [17]. The proposed CPW-to-slotline transition provides three feed modes: CPW feed, LS feed and RS feed, and is utilized to feed a wideband Vivaldi notched monopole, which is studied in [12]. In this case, the reconfigurable pattern is realized by switching the feed modes in the working frequency range from 4–6 GHz. Compared to the antenna discussed in [12], smaller dimensions of feed structure are realized. Only 2 p-i-n diodes are used in the proposed design, which is less than the 4 p-i-n diodes used in [12]. As a result, the bias circuit is simpler and the parasitic parameters as well as the insertion loss introduced by p-i-n diodes are all reduced in the proposed design. A prototype of the proposed antenna is simulated and fabricated. The reflection coefficients, radiation patterns and gains of three feed modes are measured. In order to confirm the benefits of the pattern diversity in multiple antennas systems, the channel capacity of a 2×2 antenna array is measured in a typical indoor environment. Compared to the standard omni-directional dipoles, the improvement

Manuscript received January 23, 2011; revised March 21, 2011; accepted May 01, 2011. Date of publication August 12, 2011; date of current version November 02, 2011. This work was supported by the National Basic Research Program of China under Contract 2010CB327402, in part by the National High Technology Research and Development Program of China (863 Program) under Contract 2009AA011503, the National Science and Technology Major Project of the Ministry of Science and Technology of China 2010ZX03007-001-01 and Qualcomm Inc.

Y. Li, Z. Zhang, J. Zheng, and Z. Feng are with the State Key Laboratory on Microwave and Digital Communications, Tsinghua National Laboratory for Information Science and Technology, Department of Electronic Engineering, Tsinghua University, Beijing 100084, China (e-mail: zjzh@tsinghua.edu.cn).

M. F. Iskander is with the Hawaii Center for Advanced Communications (HCAC), University of Hawaii at Manoa, Honolulu, HI 96822 USA (e-mail: iskander@spectra.eng.hawaii.edu).

Color versions of one or more of the figures in this paper are available online at <http://ieeexplore.ieee.org>.

Digital Object Identifier 10.1109/TAP.2011.2164224

of spectral efficiency is achieved by using the proposed antenna in both LOS and NLOS communication scenarios.

II. ANTENNA DESIGN PRINCIPLE

A. Antenna Configuration

The configuration of the proposed antenna is shown in Fig. 1(a). As it may be seen, it is composed of an elliptical topped monopole, two Vivaldi notched slots and a typical CPW feed with two p-i-n diodes. The antenna is printed on the both sides of a $50 \times 50 \text{ mm}^2$ Teflon substrate, whose relative permittivity is 2.65 and thickness is 1.5 mm. The CPW is connected to the microstrip at the back side through vias. A 0.2 mm wide slit is etched on the ground at the front side for DC isolation. Three curves are used to define the shape of antenna, fitted to the coordinates in Fig. 1(a):

none Curve 1:

$$\left(\frac{x}{W/2}\right)^2 + \left[\frac{y - (L_4 - \alpha * \frac{W}{2})}{\alpha * \frac{W}{2}}\right]^2 = 1 \quad (1)$$

where $L_4 - \alpha * W/2 \leq y \leq L_4$, and $\alpha = 0.4$.
none Curve 2 [18]:

$$y = C_1 e^{c \cdot x} + C_2 \quad (2)$$

where $C_1 = 14$, $C_2 = 0.26$, $c = 0.16$. Values of these parameters are chosen after optimization. Curve 3 and curve 2 are symmetrical along X axis.

B. Compact CPW-Slot Transition

In order to achieve reconfigurable patterns, a switchable CPW-to-slotline transition with 2 p-i-n diodes is used as shown in Fig. 1(b). This feed structure is able to switch from CPW feed to slotline feed by controlling the bias voltage of p-i-n diodes. The working configurations of the two p-i-n diodes (PIN 1 and PIN 2) are listed in Table I. When both p-i-n diodes are in the state of OFF, the elliptical topped monopole is fed through a typical CPW and a nearly omni-directional radiation pattern is achieved in XZ plane. When PIN 1 is OFF and PIN 2 is ON, the right slotline is shorted. The left Vivaldi notched slot is fed through the left slotline of the CPW, and a unidirectional radiation pattern is formed along the -X axis. In the same way, when PIN 1 is ON and PIN 2 is OFF, a unidirectional beam along the +X axis is achieved in the right Vivaldi notched slot through the Right Slot (RS) feed. As a result, the reconfigurable patterns are realized by switching the modes in the CPW with two p-i-n diodes.

The proposed CPW-to-slotline transitions are designed in a compact size to reduce the overall dimensions of the antenna. An equivalent transmission line model is used to explain the feed transition and the p-i-n diode is expressed as perfect conductor for ON state and open circuit for the OFF state. Fig. 2(a) shows the typical CPW feed, the length of L_5 is tuned to match the radiation resistance R_{monopole} of monopole from 50Ω at the feed port. When a slotline on either side of the CPW is

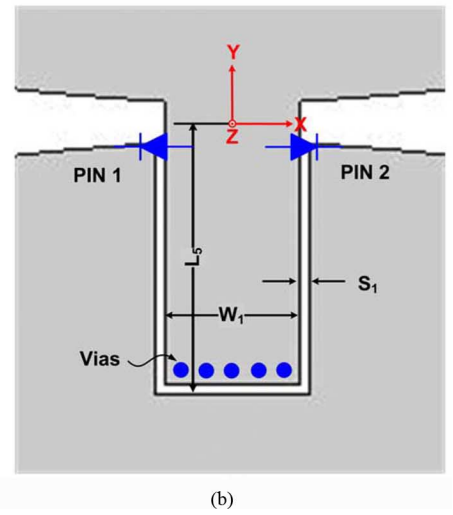
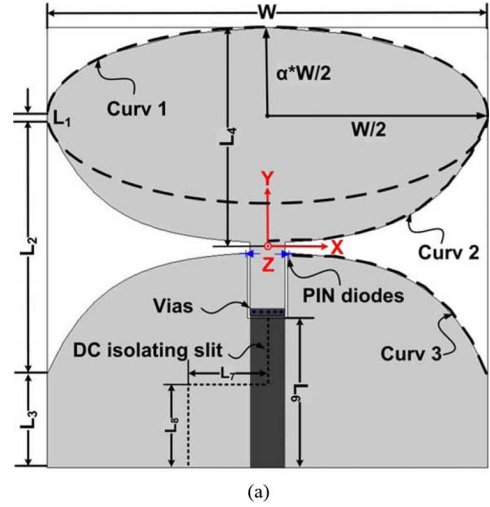


Fig. 1. Geometry and configuration of the proposed antenna. (a) Front view. (b) Detailed view of feed structure.

TABLE I
WORKING CONFIGURATION OF PIN 1 AND PIN 2

| PIN 1 | PIN 2 | Feed |
|-------|-------|------|
| OFF | OFF | CPW |
| OFF | ON | LS |
| ON | OFF | RS |

shorted by p-i-n diode, the feed diagram and equivalent transmission line model of RS feed are depicted in Fig. 2(b). The right slotline is used to feed the Vivaldi notched slot, and the shorted left slotline works as a matching branch. Some related approaches are given in [13] but the proposed method is significantly different as we don't use any extra matching structures. The shorted branch which is less than a quarter of wavelength serves as a shunt inductance and its value is determined by its length. As an improvement from the matching discuss in [16], the locations of p-i-n diodes are not fixed, as shown in Fig. 3. Therefore, the value of shunt inductance $jZ_{\text{slot}} \tan[\beta \text{slot}(L_1 - L_p)]$ can be tuned for a better matching. As a result and by optimizing the length of L_5 and L_p , the radiation resistance R_{Vivaldi}

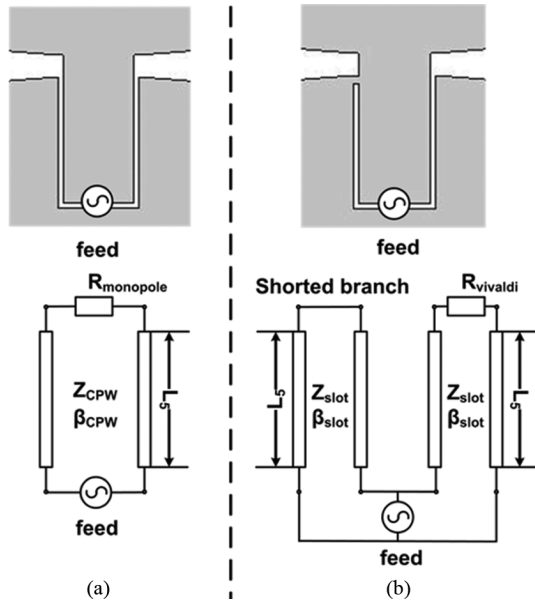


Fig. 2. Feed diagram and equivalent transmission line model. (a) CPW feed (b) RS feed.

will be well matched to 50Ω . What is more important is the fact that we only use two p-i-n diodes to control the transition instead of 4 as described in [12]. Therefore, smaller dimension of antenna is realized by using compact feed and simple bias circuit. To help evaluate the developed antenna one may make parametric study such as those described in [19], and conduct experimental validation as described in Sections III and IV of this paper. The values of parameters are optimized by using the software Ansoft High Frequency Structure Simulator (HFSS). The optimized values are listed in Table II.

III. ANTENNA FABRICATION AND EXPERIMENTAL RESULTS

In order to validate the design of the compact switchable CPW-to-slotline transition, a prototype of the proposed antenna with bias circuit is built and tested, as shown in Fig. 4. The selected p-i-n diode is Agilent HPND-4038 beam lead PIN diode, with acceptable performance in a wide 1–10 GHz bandwidth. When the p-i-n diode is forward-biased, it can be treated as a series resistance. The insertion loss introduced by p-i-n diodes is approximately 0.3 dB at its typical bias current of 5–10 mA. That is to say, the efficiency decreases 0.3 dB by using p-i-n diodes. When the p-i-n diode is reverse-biased, on the other hand, it is replaced by a series capacitance of approximately 0.06 pF, which will shift the working frequency of the antenna but with less insertion loss. As a result, the insertion loss mainly comes from the p-i-n diodes at ON state for CPW mode. Clearly, a reduced number of p-i-n diodes will reduce the insertion loss and improve the performance of the systems. The detailed bias configuration of p-i-n diodes is shown in Fig. 5. Specifically, Fig. 5(a) shows the 3-D view of bias circuit. The slit is etched on the front side to isolate the bias voltage of two p-i-n diodes. Several capacitances (C_s) are soldered over the slit for RF short. The radius of the vias, connecting the front and back sides, is 0.3 mm. In Fig. 5(b), the complete circuit diagram is illustrated.

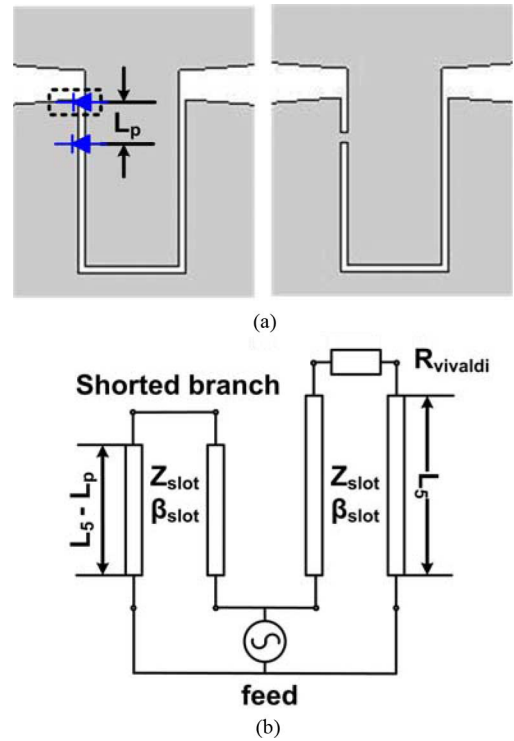


Fig. 3. Matching strategy of RS feed. (a) Feed diagram. (b) Equivalent transmission line model.

TABLE II
DETAILED DIMENSIONS OF THE PROPOSED ANTENNA

| Parameter | L_1 | L_2 | L_3 | L_4 | L_5 | L_6 |
|------------|-------|-------|-------|-------|-------|-------|
| Value (mm) | 1.74 | 28.52 | 10.74 | 25 | 8 | 16.8 |
| Parameter | L_7 | L_8 | L_p | W | l | S_1 |
| Value (mm) | 10 | 10 | 2 | 50 | 4 | 0.3 |



Fig. 4. Fabrication of the proposed antenna.

Vcontr.1, Vcontr.2 and Vcontr.3 use 3.3 V bias voltages to control the states of the two p-i-n diodes. Another capacitance is used between Vcontr.1 and the ground, in order to short the RF signal leaked from the choking inductance (L_b). Therefore, the cable of Vcontr.1 has little effect to the antenna performance. The bias circuit of p-i-n diodes is on the back side. The bias resistance (R_b) is 430Ω ; with the bias current is 7.7 mA. The RF choking inductance (L_b) is 10 nH. The RF signal shorting capacitances (C_s) are all 470 pF, and the DC block capacitances

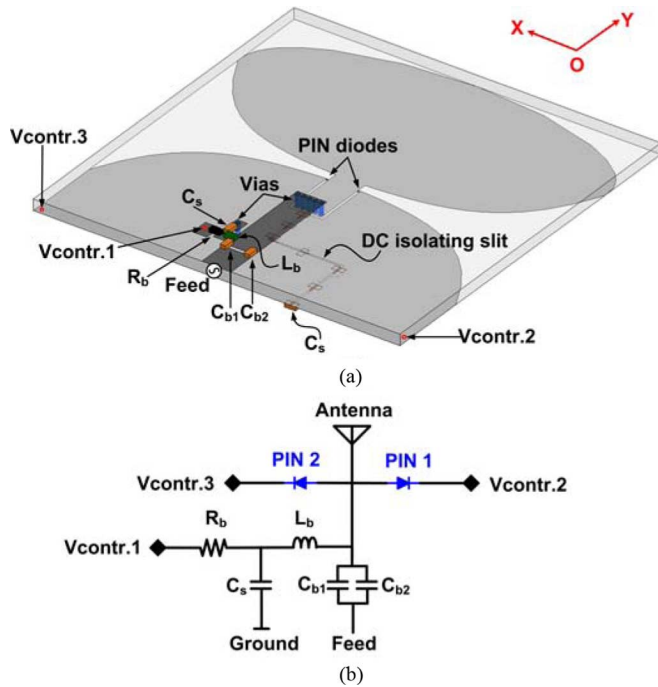


Fig. 5. Bias configuration of p-i-n diodes. (a) 3-D view. (b) Back view.

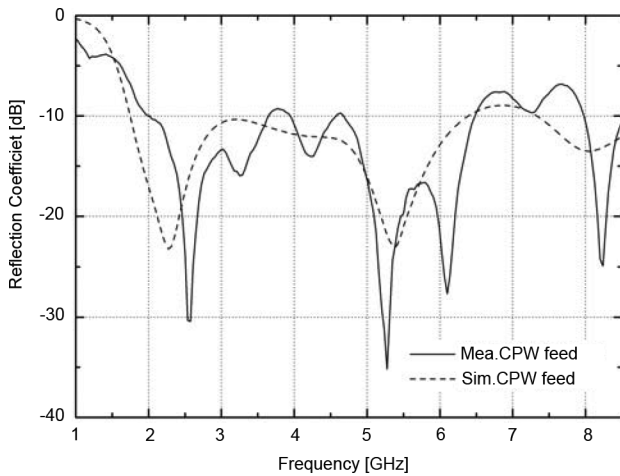


Fig. 6. Simulated and measured reflection coefficients of CPW feed.

(C_{b1} and C_{b2}) are 20 pF each. All the measurements were taken using an Agilent E5071B network analyzer. The simulated and measured reflection coefficients of CPW feed, LS and RS feeds are shown in Figs. 6 and 7. The difference between simulated and measured results is introduced by the parasitic parameter and loss of the p-i-n diodes bias circuit. The measured -10 dB bandwidths are 2.02–6.49 GHz, 3.47–8.03 GHz and 3.53–8.05 GHz for CPW feed, LS feed and RS feed, respectively. The overlap band from 3.53 GHz to 6.49 GHz is treated as the operation frequency for reconfigurable patterns.

The measured radiation pattern in XZ and XY planes for CPW feed, LS feed and RS feed at 4, 5, 6 GHz are listed in Tables III and IV. The results are normalized by the maximum value of each mode at each frequency point. For the CPW feed,

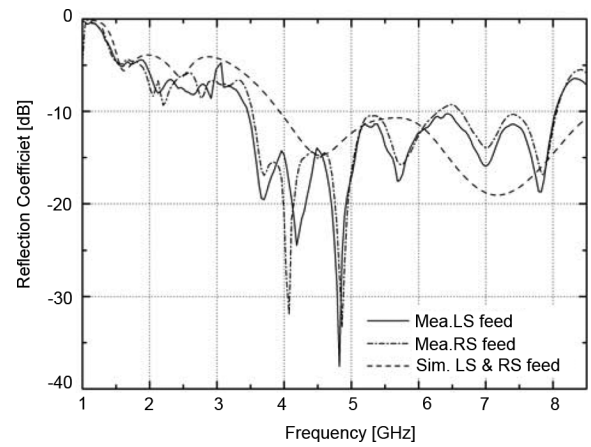


Fig. 7. Simulated and measured reflection coefficients of slotline feed.

TABLE III
MEASURED NORMALIZED RADIATION PATTERN IN XZ PLANE

| Frequency [GHz] | XZ plane: $0^\circ \rightarrow -Z, 9^\circ \rightarrow X, 180^\circ \rightarrow Z, 270^\circ \rightarrow -X$ | | |
|-----------------|--|----------|---------|
| | LS Feed | CPW feed | RS feed |
| 4 GHz | | | |
| 5 GHz | | | |
| 6 GHz | | | |

a nearly omni-directional radiation pattern is achieved in XZ plane and a doughnut shape in XY plane. For the LS or RS feed, a unidirectional beam is achieved along $-X$ or $+X$ axis, with acceptable front-to-back ratio better than 9.5 dB. The different patterns of radiation are able to be switched dynamically according to the environment, proving the pattern diversity.

The measured gains of CPW, LS and RS feed are illustrated in Fig. 8. The maximum value in the XY and XZ plane is selected as the gain of each mode. For the CPW feed, an average gain in the desired frequency range is 2.92 dBi. For the LS and RS feed, the average gains in the 4–6 GHz band are 4.29 dBi and 4.32 dBi. The improved gain is mainly contributed to the directivity of the slotline feed mode, and the diversity gain is achieved by switching the patterns.

TABLE IV
MEASURED NORMALIZED RADIATION PATTERN IN XY PLANE

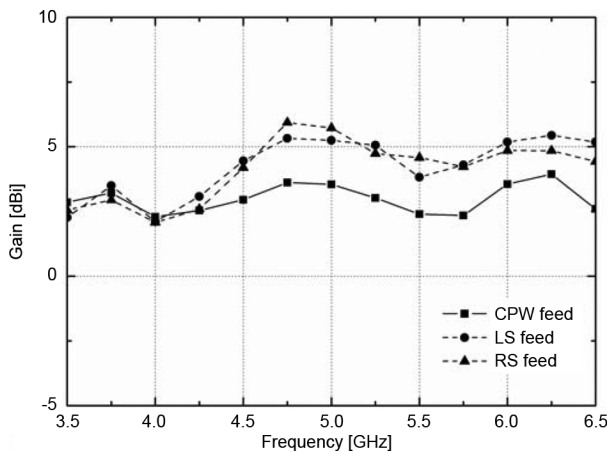
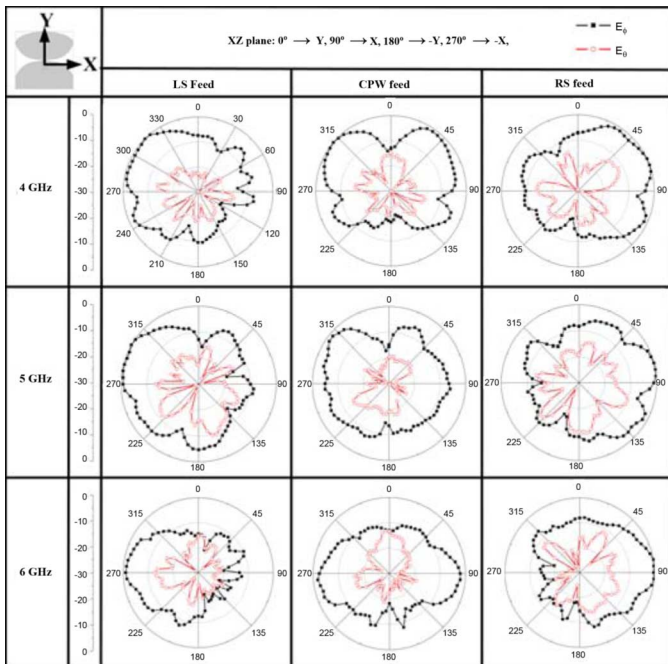


Fig. 8. Measured gains of antenna through different feed.

IV. CHANNEL CAPACITY MEASUREMENT

A. Measurement Setup

In this section, we describe the experimental procedure we used to test and validated advantages of using the developed antenna system in improving channel capacity in an indoor propagation environment. To this end, the channel capacity of a 2×2 multiple antenna system is measured. The antenna array consists of two proposed reconfigurable antennas at receive end and the reference two-dipole array at transmit end. The elements of the reference two-dipole array are arranged perpendicular to XZ plane along X axis. Each port of the two wire dipoles has a bandwidth of 3.9–5.9 GHz with reflection coefficient better than -6 dB, and mutual coupling between the two ports is lower than -25 dB over the frequency band which is achieved by tuning the distance between two elements. Also, the isolation between two proposed antennas is lower than -25 dB.

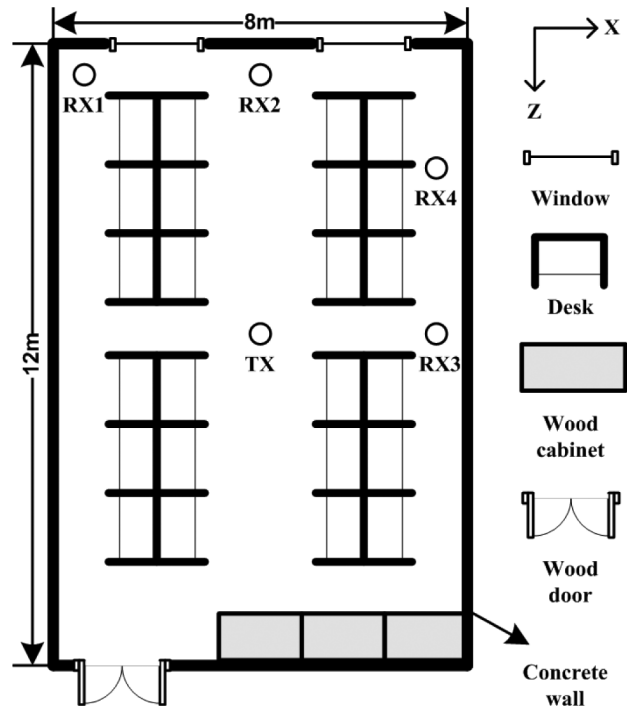


Fig. 9. Indoor environment for channel capacity measurement.

The measurement system consists of an Agilent E5071B network analyzer, which has 4 ports for simultaneous measurement, transmit antennas, receive antennas, RF switches, a computer and RF cables. The transmit antennas and the receive antennas are connected to the ports of the network analyzer, respectively. The computer controls the measurement procedure and records the measured channel responses. The measurement was carried out in a typical indoor environment in the Weiqing building of Tsinghua University, shown in Fig. 9. The framework of the room is reinforced concrete, the walls are mainly built by brick and plaster, and the ceiling is made with plaster plates with aluminium alloy framework. The heights of desk partition and wood cabinet are 1.4 m and 2.1 m. The transmit antenna array is fixed in the middle of room (TX). The receive antenna array is arranged in several typical locales which are noted as RX1-4 in Fig. 9. Here, the scenarios when the receive antenna array is arranged in RX2 and RX3 are LOS, while that is NLOS when the receive antenna array is arranged in RX1 and RX4. In the measured, the antennas used are fixed at the height of 0.8 m.

The measured data was taken in the frequency range of 4–6 GHz, with a step of 10 MHz. A total number of 201 data points/results are obtained in a typical sampling. Three configurations (CPW, LS and RS) of each element of the receiver array were switched together manually and the strongest receive signal was selected for statistics. Considering the small-scale fading effect, 5×5 grid locations for each RX position were arranged. As a result, a total number of $2 \times 201 \times 25 = 10050$ results were measured for statistics in LOS and NLOS scenario respectively. In a real scenario, the three modes of the proposed antenna can be electrically controlled by a chip depending on the strength of receiving signal.

In order to validate the effect of the proposed antennas for the systems, the channel responses of the system with another

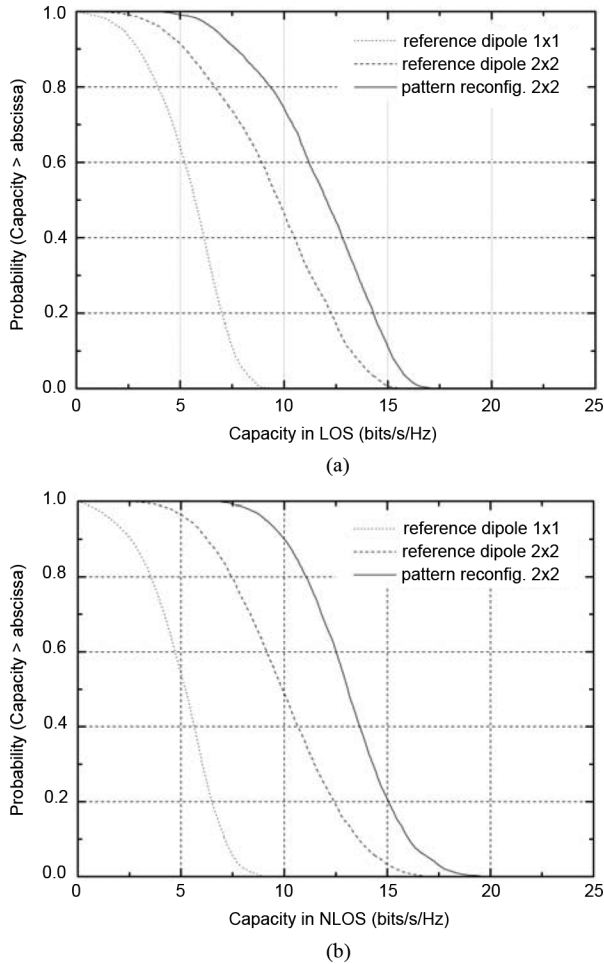


Fig. 10. CCDFs of channel capacity. (a) LOS scenario. (b) NLOS scenario.

two reference dipoles used as the receive antennas instead of the pattern reconfigurable antennas in the same measurement arrangements are measured and recorded for comparison.

In the measurement, a 2×2 channel matrix H is obtained. The channel capacity is calculated by formula (3).

$$C = \log_2 \det \left[I_{N_r} + \frac{SNR}{N_t} H_n H_n^H \right] \quad (3)$$

where N_r and N_t are the numbers of receiver and transmitter antennas. H_n is the normalized H by the received power in the reference dipole system, and $(\cdot)^H$ means the Hermitian transpose. I_{N_r} is an $N_r \times N_r$ identity matrix, and SNR is the signal-to-noise ratio. We selected the SNR when the average channel capacity is 5 bit/s/Hz in a 1×1 reference dipole system in LOS or NLOS scenario.

B. Channel Capacity Results

Fig. 10 shows the measured Complementary Cumulative Distribution Function (CCDF) of channel capacity in LOS and NLOS scenarios. The results consist of the channel capacity information of 2×2 multiple antenna system using the proposed pattern reconfigurable antennas, compared with 1×1 and 2×2 systems using reference dipoles. As listed in Table V, 2.28 bit/s/Hz and 4.13 bit/s/Hz of the average capacity improvement

TABLE V
AVERAGE AND 95% OUTAGE CHANNEL CAPACITY (BIT/S/Hz)

| Channel Capacity | Measurement Scenario | 1x1 Dipole | 2x2 Dipole | 2x2 Pattern Reconfig. |
|------------------|----------------------|------------|------------|-----------------------|
| Average | LOS | 5 | 9.46 | 11.74 |
| | NLOS | 5 | 9.93 | 13.06 |
| 95% Outage | LOS | 2.29 | 4.21 | 6.72 |
| | NLOS | 1.68 | 5.41 | 9.16 |

are achieved in LOS and NLOS scenarios, and 2.51 bit/s/Hz and 3.75 bit/s/Hz improvement for 95% outage capacities. In the NLOS scenario, the received signal is mainly contributed from reflection and diffraction of the concrete walls and the desk partitions, arriving at the direction of endfire. The diversity gain in the endfire increases the channel capacity. However, the path loss of NLOS is higher than that of LOS, and the transmitting power should be enhanced to ensure the performance of the system. Considering the insertion loss introduced from non-ideal p-i-n diodes, better performance of the proposed antenna can be achieved by using high quality switches, such as micro-electro-mechanical systems (MEMS) type switches with less insertion loss and smaller parasitic parameters.

V. CONCLUSION

A compact switchable CPW-to-slotline transition feed without extra matching structures is proposed in this paper to design a wideband reconfigurable system. CPW, LS and RS feed modes are provided to feed an elliptical topped monopole with a pair of Vivaldi notched slots for reconfigurable patterns. A nearly omni-directional pattern is achieved by feeding the monopole through CPW feed, and two endfire patterns are achieved by feeding the Vivaldi notched slots through slotline feed. An equivalent transmission line model is used to analyze the feed structure. The feed modes are controlled by only two p-i-n diodes. A prototype of the proposed antenna is fabricated and tested to prove the adequacy of the feed design. Specifically, a wide bandwidth of 3.53–6.49 GHz is achieved for reconfigurable pattern with the reflection coefficient lower than -10 dB. The radiation patterns of each feed mode are measured to demonstrate the successful achievement of the pattern diversity. The average gain improvement in the direction of endfire is better than 1.37 dB in the operation band. To prove the benefit of diversity gain, the channel capacity of a 2×2 multiple antenna system using the proposed antennas is measured in an indoor propagation environment. Compared with reference wire dipoles in the same measurement, the average and 95% outage capacities are both improved by using the proposed antennas, especially in a NLOS scenario.

REFERENCES

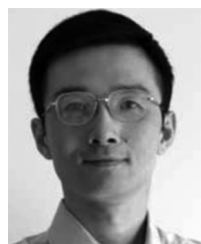
- [1] D. Piazza, P. Mookiah, M. D'Amico, and K. R. Dandekar, "Experimental analysis of pattern and polarization reconfigurable circular patch antennas for MIMO systems," *IEEE Trans. Veh. Technol.*, vol. 59, no. 5, pp. 2352–2363, Jun. 2010.
- [2] M. Sanchez-Fernandez, E. Rajo-Iglesias, O. Quevedo-Teruel, and M. L. Pablo-González, "Spectral efficiency in MIMO systems using space and pattern diversities under compactness constraints," *IEEE Trans. Veh. Technol.*, vol. 57, pp. 1637–1645, 2008.
- [3] J. D. Boerman and J. T. Bernhard, "Performance study of pattern reconfigurable antennas in MIMO communication systems," *IEEE Trans. Antennas Propag.*, vol. 56, no. 1, pp. 231–236, Jun. 2008.

- [4] G. H. Huff and J. T. Bernhard, "Integration of packaged RF MEMS switches with radiation pattern reconfigurable square spiral microstrip antennas," *IEEE Trans. Antennas Propag.*, vol. 54, no. 2, pp. 464–469, Feb. 2006.
- [5] P. Deo, A. Mehta, D. Mirshekar-Syahkal, and H. Nakano, "An HIS-based spiral antenna for pattern reconfigurable applications," *IEEE Antennas Wireless Propag. Lett.*, vol. 8, pp. 196–199, 2009.
- [6] S.-H. Chen, J.-S. Row, and K.-L. Wong, "Reconfigurable square-ring patch antenna with pattern diversity," *IEEE Trans. Antennas Propag.*, vol. 55, no. 2, pp. 492–475, Feb. 2007.
- [7] X.-S. Yang, B.-Z. Wang, W. Wu, and S. Xiao, "Yagi patch antenna with dual-band and pattern reconfigurable characteristics," *IEEE Antennas Wireless Propag. Lett.*, vol. 6, pp. 168–171, 2007.
- [8] S. Zhang, G. H. Huff, J. Feng, and J. T. Bernhard, "A pattern reconfigurable microstrip parasitic array," *IEEE Trans. Antennas Propag.*, vol. 52, no. 10, pp. 2773–2776, Oct. 2004.
- [9] J. Sarrazin, Y. Mahé, S. Avrillon, and S. Toutain, "Pattern reconfigurable cubic antenna," *IEEE Trans. Antennas Propag.*, vol. 57, no. 2, pp. 310–317, Feb. 2009.
- [10] A. C. K. Mak, C. R. Rowell, and R. D. Murch, "Low cost reconfigurable landstorf planar antenna array," *IEEE Trans. Antennas Propag.*, vol. 57, no. 10, pp. 3051–3061, Oct. 2009.
- [11] I.-Y. Tarn and S.-J. Chung, "A novel pattern diversity reflector antenna using reconfigurable frequency selective reflectors," *IEEE Trans. Antennas Propag.*, vol. 57, no. 10, pp. 3035–3042, Oct. 2009.
- [12] S.-J. Wu and T.-G. Ma, "A wideband slotted bow-tie antenna with reconfigurable CPW-to-Slotline transition for pattern diversity," *IEEE Trans. Antennas Propag.*, vol. 56, no. 2, pp. 327–334, Feb. 2008.
- [13] H. Kim, D. Chung, D. E. Anagnostou, and J. Papapolymerou, "Hard-wired design of ultra-wideband reconfigurable MEMS antenna," in *Proc. IEEE 18th Ann. Int. Symp on Personal, Indoor and Mobile Communications, PIMRC*, Sep. 3–7, 2007.
- [14] K.-P. Ma, Y. Qian, and T. Itoh, "Analysis and applications of a new CPW-slotline transition," *IEEE Trans. Microwave Theory Tech.*, vol. 47, pp. 426–432, Apr. 1999.
- [15] Y.-S. Lin and C. H. Chen, "Design and modeling of twin-spiral coplanar-waveguide-to-slotline transitions," *IEEE Trans. Microwave Theory Tech.*, vol. 48, pp. 463–466, Mar. 2000.
- [16] K. Hettak, N. Dib, A. Sheta, A. Omar, G. Y. Delisle, M. Stubbs, and S. Toutain, "New miniature broadband CPW-to-slotline transitions," *IEEE Trans. Microwave Theory Tech.*, vol. 48, pp. 138–146, Jan. 2000.
- [17] Y. Li, Z. Zhang, W. Chen, and Z. Feng, "Polarization reconfigurable slot antenna with a novel compact CPW-to-Slotline transition for WLAN application," *IEEE Antennas Wireless Propag. Lett.*, vol. 9, pp. 252–255, 2010.
- [18] J. Shin and D. H. Schaubert, "A parameter study of stripline-fed Vivaldi notch-antenna arrays," *IEEE Trans. Antennas Propag.*, vol. 47, pp. 879–886, May 1999.
- [19] Y. Li, Z. Zhang, Z. Feng, M. Iskander, and R. Li, "A wideband pattern reconfigurable antenna with compact switchable feed structure," in *Proc. Int. Conf. on Microwave and Millimeter Wave Technology*, Chengdu, China, May 2010, pp. 1–4.



Yue Li was born in Shenyang, Liaoning Province, China, in 1984. He received the B.S. degree in telecommunication engineering from Zhejiang University, Zhejiang, China, in 2007. He is currently working toward Ph.D. degree in electrical engineering from Tsinghua University, Beijing, China.

His current research interests include antenna design and theory, particularly in reconfigurable antennas, electrically small antennas and antenna in package.



Zhijun Zhang (M'00–SM'04) received the B.S. and M.S. degrees from the University of Electronic Science and Technology of China, in 1992 and 1995 respectively, and the Ph.D. from Tsinghua University, China, in 1999.

In 1999, he was a Postdoctoral Fellow with the Department of Electrical Engineering, University of Utah, where he was appointed a Research Assistant Professor in 2001. In May 2002, he was an Assistant Researcher with the University of Hawaii at Manoa, Honolulu. In November 2002, he joined Amphenol

T&M Antennas, Vernon Hills, IL, as a Senior Staff Antenna Development Engineer and was then promoted to the position of Antenna Engineer Manager. In 2004, he joined Nokia Inc., San Diego, CA, as a Senior Antenna Design Engineer. In 2006, he joined Apple Inc., Cupertino, CA, as a Senior Antenna Design Engineer and was then promoted to the position of Principal Antenna Engineer. Since August 2007, he has been has been a Professor in the Department of Electronic Engineering, Tsinghua University, Beijing, China.



Jianfeng Zheng received the B.S. and Ph.D. degrees from Tsinghua University, Beijing, China, in 2002 and 2009, respectively.

He is currently an Assistant Researcher with the State Key Laboratory on Microwave and Digital Communications, Tsinghua University. His current research interests include spatial temporal signal processing, MIMO channel measurements and antenna arrays for MIMO communications.



Zhenghe Feng (SM'85) received the B.S. degree in radio and electronics from Tsinghua University, Beijing, China, in 1970.

Since 1970, he has been with Tsinghua University, as an Assistant, Lecture, Associate Professor, and Full Professor. His main research areas include numerical techniques and computational electromagnetics, RF and microwave circuits and antenna, wireless communications, smart antenna, and spatial temporal signal processing.



Magdy F. Iskander (F'91) is the Director of the Hawaii Center for Advanced Communications (HCAC), College of Engineering, University of Hawaii at Manoa, Honolulu, Hawaii (<http://hcac.hawaii.edu>). He is also a Co-director of the NSF Industry/University joint Cooperative Research Center between the University of Hawaii and four other universities in the US. From 1997–99 he was a Program Director at the National Science Foundation, where he formulated and directed a "Wireless Information Technology" Initiative in

the Engineering Directorate. He spent sabbaticals and other short leaves at Polytechnic University of New York; Ecole Supérieure D'Electricité, France; UCLA; Harvey Mudd College; Tokyo Institute of Technology; Polytechnic University of Catalunya, Spain; University of Nice-Sophia Antipolis, and Tsinghua University, China. He authored a textbook *Electromagnetic Fields and Waves* (Prentice Hall, 1992; and Waveland Press, 2001); edited the *CAEME Software Books*, Vol. I, 1991, and Vol. II, 1994; and edited four other books on *Microwave Processing of Materials*, all published by the Materials Research Society, 1990–1996. He has published over 200 papers in technical journals, holds eight patents, and has made numerous presentations in International conferences. He is the founding editor of the journal *Computer Applications in Engineering Education* (CAE), published by Wiley. His research focus is on antenna design and propagation modeling for wireless communications and radar systems, and in computational electromagnetics.

Dr. Iskander received the 2010 University of Hawaii Board of Regents' Medal for Excellence in Teaching, the 2010 Northrop Grumman Excellence in Teaching Award, the 2011 Hi Chang Chai Outstanding Teaching Award, and the University of Utah Distinguished Teaching Award in 2000. He also received the 1985 Curtis W. McGraw ASEE National Research Award, 1991 ASEE George Westinghouse National Education Award, 1992 Richard R. Stoddard Award from the IEEE EMC Society. He was a member of the 1999 WTEC panel on "Wireless Information Technology-Europe and Japan," and chaired two International Technology Institute panels on "Asian Telecommunication Technology" sponsored by DoD in 2001 and 2003. He spent sabbaticals and other short leaves at Polytechnic University of New York; Ecole Supérieure D'Electricité, France; UCLA; Harvey Mudd College; Tokyo Institute of Technology; Polytechnic University of Catalunya, Spain; University of Nice-Sophia Antipolis, and Tsinghua University, China.